Rapid Synthesis of Phase-Engineered Tungsten Carbide Electrocatalysts via Flash Joule Heating for High-Current-Density Hydrogen Evolution

Amirarsalan Mashhadian[1], Shiwen Wu[1], Yun Hao[1], Mahdi Mosadegh[1], Kyeongjae Cho[2], Majid Minary-Jolandan[1*], Guoping Xiong[1*]

[1] Department of Mechanical Engineering, The University of Texas at Dallas, 800 W Campbell Rd, Richardson, TX 75080, United States

[2] Department of Material Science Engineering, The University of Texas at Dallas, 800 W Campbell Rd, Richardson, TX 75080, United States

* Corresponding Author: Majid.Minary@utdallas.edu

* Corresponding Author: Guoping.Xiong@utdallas.edu

Abstract

Fabricating durable and high-performance electrocatalysts operating at high current densities for industrial acidic hydrogen evolution remains a daunting challenge. Tailoring the phase composition of electrocatalysts is a promising strategy to harness synergistic effects and improve charge transfer, thereby optimizing their performance. This work presents a fast, green method based on flash joule heating (FJH) to synthesize phase-engineered tungsten carbide electrocatalysts for the acidic hydrogen evolution reaction (HER) at high current densities. Tungsten carbide electrodes with varying FJH treatment durations (3, 10, 30, and 60 seconds) are fabricated to fine-tune the mixture of tungsten monocarbide (WC) and tungsten semicarbide (W_2C) phases. Results show that samples with a 30-second treatment (TC-3) exhibit an optimal balance between these phases, leading to a low overpotential of 387 mV at a high current density of 4 A/cm^2. Notably, the TC-3 electrocatalysts remain stable for over 6 days at 4 A/cm^2 due to their controlled phases and excellent corrosion-resistant properties. This work highlights a new method to fabricate cost-effective, high-performance tungsten carbide electrocatalysts with well-controlled phase compositions.

Keywords: Acidic Hydrogen Evolution Reaction, Tungsten Carbides, Flash Joule Heating, Phase Engineering

1. Introduction

The excessive reliance on fossil fuels has led to severe environmental pollution and global warming, creating an urgent need for renewable and clean energy sources as alternatives[1,2]. Hydrogen has emerged as a promising energy carrier for meeting clean energy demands due to its high energy density and environmentally benign properties[3]. Electrocatalytic hydrogen production offers an economical and efficient approach to achieving a closed carbon cycle[4]. Currently, platinum (Pt) stands as the most efficient electrocatalyst for the hydrogen evolution reaction (HER) in acidic media due to its favorable electronic structure, which facilitates moderate binding energy with hydrogen ions, a crucial attribute for achieving efficient catalytic performance[5,6]. The Pt catalysts for the HER in acidic media suffer from two major limitations including their high cost, which hinders large-scale production[7], and performance deterioration at high current densities due to catalyst restructuring issues[8,9].

Transition metal (e.g., Mo, W) carbides (TMCs) have been considered as promising alternatives to Pt catalysts for HER due to their low cost and Pt-like electronic structures[10]. Particularly, tungsten carbide shows exceptional performance (e.g., low overpotential and long-term stability) at high current densities stemming from its corrosion resistance nature and high electronic conductivity[11]. Tungsten carbide possesses multiple phases, such as tungsten monocarbide (WC) and tungsten semi-carbide (W_2C), exhibiting diverse electrocatalytic properties for HER[12]. The synergetic effects of these phases can lead to improved HER activity by modulating the hydrogen adsorption energy due to different interactions and charge transfer mechanisms at the phase interfaces[13,14]. Despite recent studies on molybdenum carbide phase optimization in alkaline media[15], little work has been reported on optimizing tungsten carbide phases for

hydrogen evolution reaction (HER) at high current densities (> 3 A/cm^2) in acidic media[16]. Thus, optimizing the composition of different tungsten carbide phases is crucial to improving the HER activity of the catalyst.

In this study, a rapid, cost-effective, and environment-friendly method based on flash Joule heating (FJH) has been implemented to fabricate tungsten carbide catalysts with optimized phases, as efficient alternatives to Pt, for high-performance acidic hydrogen production at industrial-level current densities. A series of tungsten carbide electrodes were synthesized with different FJH durations (3, 10, 30, and 60 seconds) to tailor the phase composition of WC and W_2C. The results revealed that the sample synthesized for 30 seconds (denoted as TC-3) exhibited the optimal performance at a high current density of 4 A/cm^2, attributed to the optimized ratio of WC to W_2C phases and resulting synergistic effects. Remarkably, the TC-3 sample demonstrated exceptional stability, maintaining its performance for over 6 days of continuous operation at 4 A/cm^2, ascribed to the inherent corrosion-resistant properties of tungsten carbide and strong tungsten-carbon bonding. This work paves the way for the scalable production of cost-effective and robust tungsten carbide catalysts outperforming Pt, particularly for high-current-density industrial hydrogen production applications where high throughput and long-term stability are crucial.

2. Experimental section

2.1. Preparation of the tungsten carbide electrode

Carbon papers (MGL 190, Fuel Cell Earth Co.) were cleaned in a sonication process using acetone (Sigma Aldrich), followed by 2-propanol (Fisher Scientific Co.), and then deionized (DI) water. Subsequently, the surface of carbon papers was treated by air plasma (Harrick Plasma) at a medium intensity of 10.5 W for 1 minute to become hydrophilic. A 0.5 M sodium tungstate

(Na_2WO_4, STREM Co.) solution was prepared by dissolving 1649.3 mg of the salt precursor in 10-mL DI water with the assistance of sonication for 15 minutes (Fig. 1a). Carbon paper substrates (8mm×20mm) were immersed in the prepared solution for 20 minutes and then dried for 30 minutes at 60 ºC in an oven. To synthesize tungsten carbides, the prepared samples were sandwiched between two pieces of graphite felts, and the temperature was ramped up to 900 ºC by FJH within one second (Fig. 1b and c). Tungsten carbides were synthesized for durations of 3, 10, 30, and 60 seconds, corresponding to samples denoted as TC-1, TC-2, TC-3, and TC-4, respectively. Following the fabrication of tungsten carbide on carbon paper substrates, the samples were washed multiple times with ethanol and DI water to remove any salt residues.

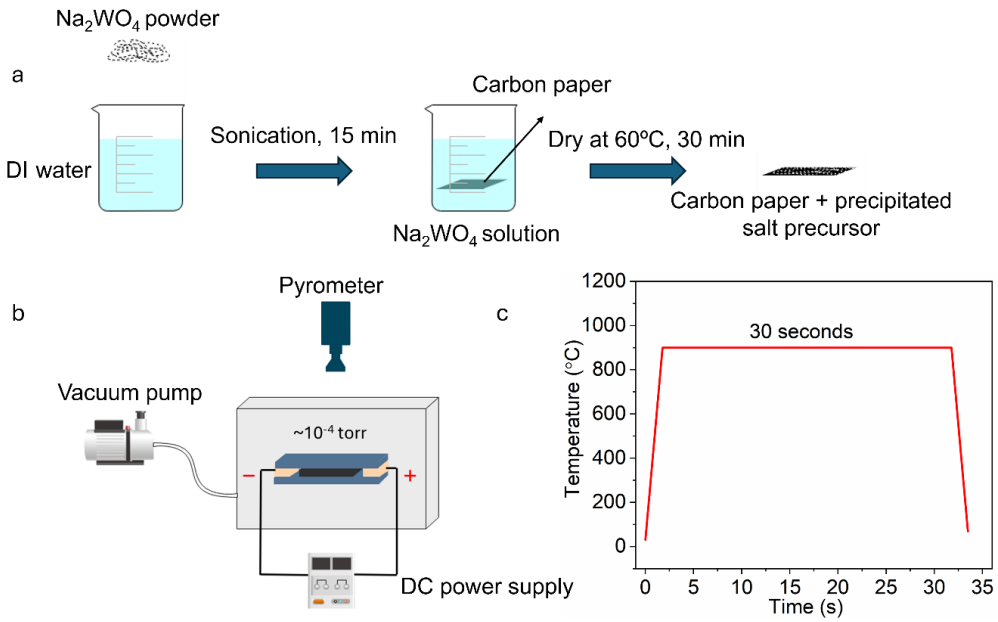

Figure 1- (a) Schematic of the fabrication process of tungsten carbide electrocatalyst using a carbon paper substrate, (b) schematic of the FJH experimental setup to fabricate tungsten carbide electrocatalyst, (c) Temperature-time curves during the FJH process.

2.2. Characterization

The phase composition of the samples was analyzed by X-ray diffraction within the range from 30º to 70º (XRD, Bruker D8 P-XRD) using Cu Kα radiation (λ = 1.5418 Å). The morphology of as-prepared tungsten carbides was studied by scanning electron microscopy (SEM, Zeiss Supra 40). The chemical analysis of the samples was conducted by high-resolution X-ray photoelectron spectroscopy (XPS, Versa probe II). The pass energy and energy step size for XPS were chosen to be 50 eV and 0.1 eV, respectively. Raman spectra were collected using Horiba Raman microscope with an excitation laser of 532 nm at a magnification of 50X.

2.3. Electrochemical measurements

A three-electrode configuration was used for the electrochemical measurement in 0.5 M H_2SO_4 aqueous electrolyte solution (pH ≈ 0.3). In the electrochemical tests, voltage and current were controlled and measured by a potentiostat (Gamry interface 1010E). A graphite rod and an Ag/AgCl electrode were employed as counter and reference electrodes, respectively. The activation of tungsten carbide electrodes was implemented by performing cyclic voltammetry (CV) for 50 cycles. Linear scan voltammetry (LSV) was carried out with a scan rate of 2 mV/s. The stability tests were conducted by using chronopotentiometry techniques. All of the potential values are reported after *iR* compensation and versus reversible hydrogen electrode (RHE), which were calculated using the following equation[17]: $E_{\mathrm{RHE}} = E_{\mathrm{Ag/AgCl}} + E°_{\mathrm{Ag/AgCl}} + (0.059 \times \mathrm{pH})$. In the above equation, E_{RHE} represents the calculated potential versus the RHE, $E_{\mathrm{Ag/AgCl}}$ denotes the measured potential relative to the Ag/AgCl reference electrode, and $E°_{\mathrm{Ag/AgCl}}$ is the standard electrode potential ($E°$ = 0.197 V at 25 ºC) for the Ag/AgCl electrode.

3. Results and discussion

The XRD patterns of the samples prepared by different FJH durations (i.e., TC-1, TC-2, TC-3, and TC-4) are shown in Fig. 2a and coincide with those reported in prior work[18], confirming the successful synthesis of tungsten carbides in all these samples. Moreover, varying the FJH duration effectively influences the phase compositions such as tungsten (W), WC, and W_2C phases in the products and their relative quantities. As shown in Fig. 2a, TC-1 exhibits characteristic peaks located at 34.6º, 38.1º, and 39.5º corresponding to the hexagonal W_2C phase[19], while TC-2, TC-3, and TC-4 display characteristic peaks for both hexagonal WC and W_2C phases. This phenomenon suggests that the ratio of WC to W_2C peaks increases with the FJH treatment duration, and the characteristic peaks associated with the elemental W disappear when the fabrication duration is longer than 3 s. We believe that the carbon source for the synthesis of tungsten carbides originate from the carbon fiber substrate itself, a similar phenomenon observed in the prior work[20].

Raman spectroscopy provides additional information about the structures of FJH-synthesized samples. For TC-1, a characteristic peak is observed at around 686 cm^{-1}, corresponding to the W-C stretching mode. However, this peak becomes broader and weaker for TC-2, TC-3, and TC-4, as the phase-pure WC emerges[21]. The peak located at approximately 250 cm^{-1} is ascribed to oxygen bonding (i.e., WC-O), which is due to the oxidation of the sample surface in air. The W-C bonding is further confirmed by XPS data (Fig. S1-S4), with no detectable oxygen bonding to tungsten or carbon, ruling out the formation of tungsten oxides. Furthermore, three main characteristic peaks are observed in all the samples at approximately 1340, 1594, and 2700 cm^{-1}, attributed to the D-band (diamond-like carbon), G-band (graphitic carbon), and 2D-band (layered structure of graphite or graphene), respectively (Fig. S5)[22]. The relative intensity ratio of the G-band to D-band, indicative of the graphitic degree of the carbon content, exhibits a direct

relationship with the FJH synthesis duration of tungsten carbides, suggesting a more well-defined crystalline structure with increasing FJH durations[23,24].

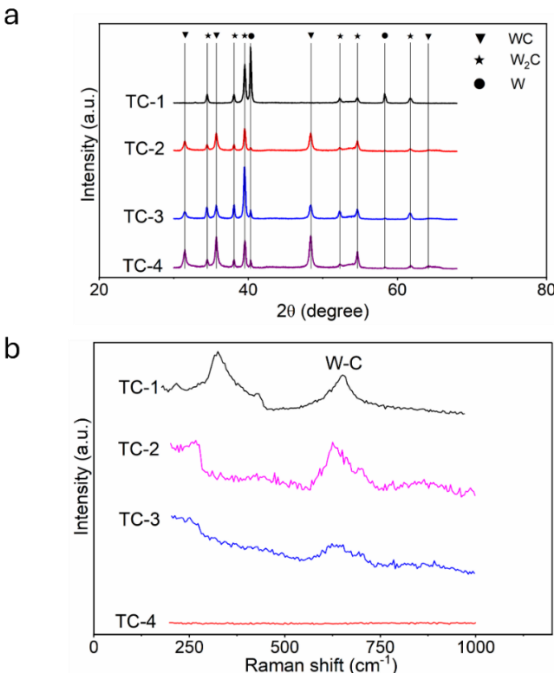

Figure 2- (a) XRD patterns and (b) Raman spectra of tungsten carbide electrocatalysts with different FJH durations.

The microstructural morphology of the synthesized tungsten carbide samples by FJH was investigated by SEM. Specifically, TC-1 exhibits the uniform formation of densely connected nanoparticles with sizes ranging from 30 to 50 nm (Fig. 3a and b). For TC-2, connected nanoparticles ranging from 50 to 260 nm in size cover the entire carbon fiber surface forming a porous-like structure (Fig. 3c and d). Moreover, a porous structure comprised of uniform nanoparticles with an average size of approximately 70 nm forms on the surface of the TC-3 catalyst (Fig. 3e and f), resulting in a higher surface area and more active sites for the HER compared to the other catalysts. In addition, the element distribution of tungsten is uniform throughout the catalysts, suggesting well-dispersed active sites for effective HER (Fig. S6). As

shown in Figs. 3g and h, a dense layer is formed on the surface of carbon fiber, indicating the tungsten carbide particles are sintered to be interconnected, which can hinder effective HER.

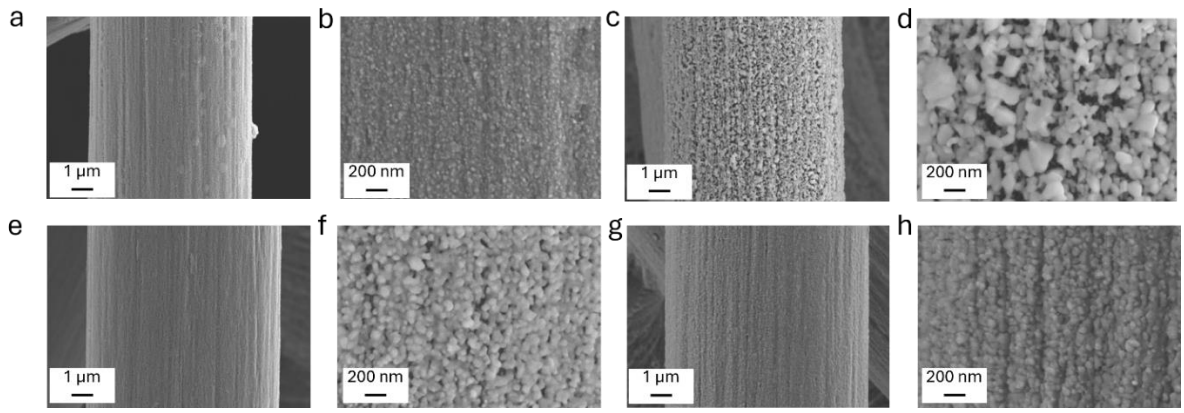

Figure 3- SEM images of tungsten carbide electrocatalysts with different FJH durations: (a, b) TC-1 (3 s), (c, d) TC-2 (10 s), (e, f) TC-3 (30 s), (g, h) TC-4 (60 s).

The HER performance of the synthesized tungsten carbide samples with different FJH durations was evaluated in an acidic environment using LSV. Fig. 4a depicts the polarization curves obtained in 0.5 M H_2SO_4 for all fabricated tungsten carbide samples and a commercial Pt/C catalyst. The overpotential of TC-4 at a current density of 10 mA/cm^2 was determined to be 180.97 mV, which is the lowest among the tungsten carbide samples but higher than that (44.19 mV) of Pt/C. The overpotentials of TC-1, TC-2, and TC-3 catalysts were 239.02 mV, 194.98 mV, and 187.57 mV, respectively, indicating a decrease in overpotential with increasing FJH synthesis durations. This trend may be attributed to the co-existence of three active components (W, WC, and W_2C) and their potential synergistic effects, resulting in modulated hydrogen binding energy and enhanced charge transfer kinetics[25]. At a high current density of 4 A/cm^2, TC-3 exhibited the best performance (η = 387 mV) among the fabricated tungsten carbide samples, significantly outperforming TC-1 (469.73 mV) and TC-4 (418.39 mV). Remarkably, TC-3 also outperformed Pt/C at current densities exceeding 630 mA/cm^2, demonstrating its exceptional kinetics at high

current densities. The superior hydrogen evolution performance of TC-3 suggests the importance of the synergetic effect between the two phases (i.e., W_2C and WC) and especially their improved interface charge transfer.

The Tafel plot analysis (Fig. 4b) provides further insights into the kinetics of the HER for the synthesized tungsten carbide samples. The Tafel slopes of TC-1 to TC-4 fall within a similar range of 53.7, 51.8, 53.7, and 60.5 mV/dec, respectively. These values are significantly larger than the Tafel slope of 29.53 mV/dec observed for the Pt/C, suggesting more sluggish kinetics at low current densities compared to Pt/C. Based on the Tafel plot data, the rate-determining step for the tungsten carbide samples is likely the Heyrovsky reaction (electrochemical desorption of H_2) at low current densities[15]. Furthermore, as shown in Fig. 4c, the Tafel slopes of the tungsten carbide samples remain below 120 mV/dec across different current density ranges, indicating rapid kinetic processes even at high current densities. Notably, TC-3 exhibits higher rapid kinetics compared to TC-1, TC-2, and TC-4, which can be attributed to a lower reaction resistance of TC-3 compared to the other samples. Such a lower reaction resistance of TC-3 can be linked to the optimized compositions of WC and W_2C phases. It should be noted that the HER kinetics for all the tungsten carbide samples appear faster than that of Pt/C at current densities larger than 100 mA/cm^2, indicating the superior HER performance of FJH-fabricated tungsten carbide catalysts operating at high current densities.

Long-term stability is a crucial performance indicator for HER catalysts, particularly in acidic environments. The durability of the optimized TC-3 catalyst was evaluated by conducting stability tests at a high current density of 4 A/cm^2. Remarkably, the TC-3 catalyst demonstrates exceptional stability, maintaining a constant potential over an extended period of continuous electrolysis exceeding 150 hours (> 6 days), as evident from Fig. 4d. The exceptional

performance of TC-3 (e.g., long-term stability and low overpotential) at an ultrahigh current density of 4 A/cm^2 stands among the best electrocatalysts reported in prior work for acidic HER (Table S1)[26–29]. The outstanding stability of the TC-3 catalyst can be attributed to the inherent corrosion resistance of tungsten carbides and the strong bonding between tungsten carbide and the substrate formed during the synthesis process.

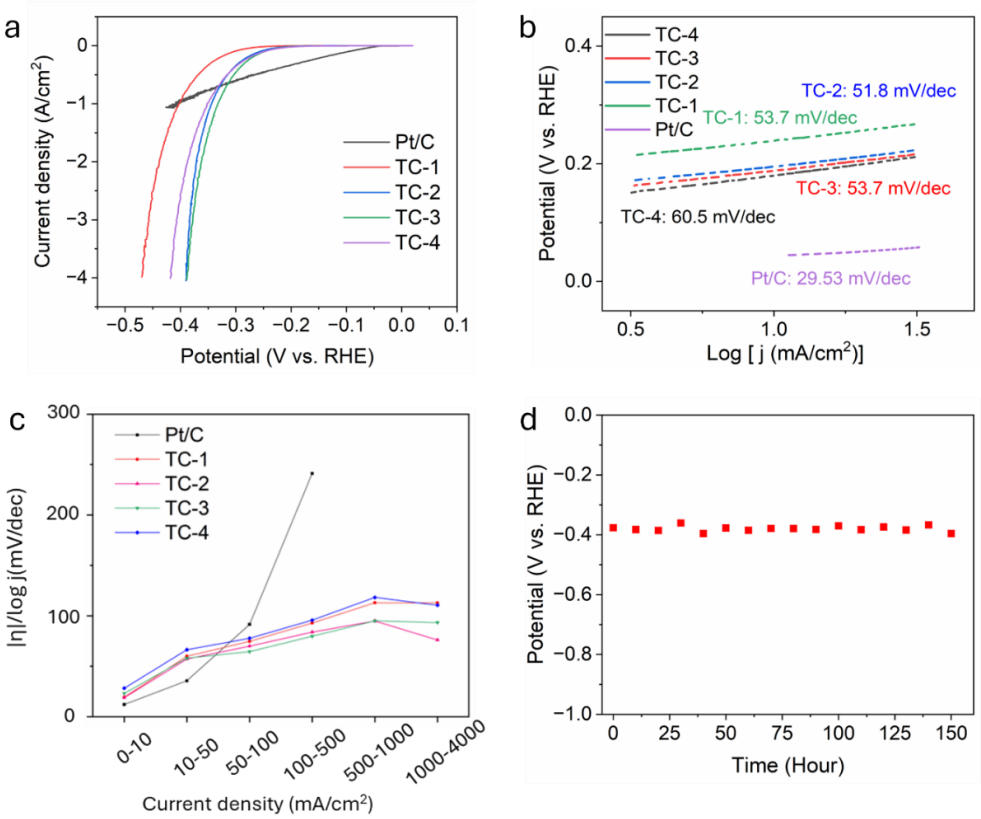

Figure 4 - Comparative performance of Pt/C electrocatalyst and tungsten carbide electrocatalysts with different FJH durations: (a) polarization curves, (b) Tafel curves, (c) ratios of $\Delta\eta/\Delta\log|j|$, (d) long-term stability test for TC-3 electrocatalyst at 4 A/cm^2 with iR compensation.

4. Conclusion

A facile and rapid FJH method has been successfully employed to synthesize tungsten carbide electrocatalysts with well-controlled phase compositions, demonstrating exceptional acidic HER

catalytic activity, particularly at high current densities. The tungsten carbide electrocatalysts were synthesized with varying FJH durations to tailor the phase composition, enabling the coexistence of WC and W_2C phases and capitalizing on their potential synergistic effects. Notably, the TC-3 catalyst outperformed other tungsten carbide catalysts, with a low overpotential (387 mV) achieved at a high current density of 4 A/cm^2. Moreover, the TC-3 catalyst showcases its exceptional stability by maintaining a constant potential during continuous electrolysis for over 150 hours (>6 days), which sets it among the best acidic HER electrocatalysts. This outstanding combination of high efficiency and exceptional stability renders the TC-3 catalyst a promising candidate for industrial-scale hydrogen production applications.

Acknowledgment

G.X. thanks the University of Texas at Dallas startup fund.

Conflict of interest

The authors declare no conflict of interest.

References

1. O. Ellabban, H. Abu-Rub, and F. Blaabjerg, Renew. Sustain. Energy Rev. 39 (2014): 748–764.
2. S. Chu and A. Majumdar, Nature 488, no. 7412 (2012): 294–303.
3. N. Sazali, Int. J. Hydrogen Energy 45 (2020): 18753–18771.
4. Z. Abdin et al., Renew. Sustain. Energy Rev. 120 (2020): 109620.
5. W. kong et al., Nano Res. 16 (2023): 195–201.
6. A. H. Shah, C. Wan, Y. Huang, and X. Duan, J. Phys. Chem. C 127 (2023): 12841–12848.
7. Z. W. Seh et al., Science 355, no. 6321 (2017): eaad4998.
8. D. Liu et al., Small 17, no. 50 (2021): 2007557.
9. W. Sheng et al., Nat. Commun. 6 (2015): 5848.
10. H. Jun, S. Kim, and J. Lee, Korean J. Chem. Eng. 37 (2020): 1317–1330.

11. J. Huang et al., Sustain. Energy Fuels 4 (2020): 1078–1083.
12. F. Harnisch, G. Sievers, and U. Schröder, Appl. Catal. B Environ. 89 (2009): 455–458.
13. Y.-L. T. Ngo et al., Chem. Eng. J. 450 (2022): 137915.
14. X. Zhang et al., Chem. Eng. J. 408 (2021): 127270.
15. C. Li et al., Nat. Commun. 13 (2022): 3338.
16. R. Riedmayer et al., Energy & Fuels 37 (2023): 8614–8623.
17. L. Zan et al., J. Alloys Compd. 869 (2021): 159324.
18. S. Emin et al., Appl. Catal. B Environ. 236 (2018): 147–153.
19. Y. Ling et al., Int. J. Hydrogen Energy 46 (2021): 9699–9706.
20. S. Meng et al., Catal. Today 402 (2022): 266–275.
21. Z. Chen et al., Nano Energy 68 (2020): 104335.
22. K. Kornaus et al., Polish J. Chem. Technol. 18 (2016): 84–88.
23. I. Tallo et al., Carbon N. Y. 49 (2011): 4427–4433.
24. J. L. Lu et al., J. Power Sources 202 (2012): 56–62.
25. X. Fan et al., Appl. Catal. B Environ. 318 (2022): 121867.
26. I. K. Mishra et al., Energy Environ. Sci. 11 (2018): 2246–2252.
27. Z. Zheng et al., Nat. Commun. 11 (2020): 3315.
28. Y. Chen et al., J. Am. Chem. Soc. 139, no. 36 (2017): 12370–12373.
29. R. Liu et al., Adv. Mater. 33, no. 44 (2021): 2103533.